Impact of cationic polystyrene nanoparticles (PS-NH_2) on early embryo development of *Mytilus galloprovincialis*: effects on shell formation

Teresa Balbi[1], Giulia Camisassi[1], Michele Montagna[1], Rita Fabbri[1], Silvia Franzellitti[2], Cristina Carbone[1], Kenneth Dawson[3], Laura Canesi[1*]

[1]Department of Earth, Environment and Life Sciences (DISTAV), University of Genova, Genova, Italy.

[2]Department of Biological, Geological and Environmental Sciences, University of Bologna, Campus of Ravenna, Ravenna, Italy

[3]Centre for BioNanoInteractions, School of Chemistry and Chemical Biology, University College Dublin, Ireland

* Corresponding Author
Laura.Canesi@unige.it
DISTAV-Dipartimento di Scienze della Terra, dell'Ambiente e della Vita,
Università di Genova
Corso Europa 26
16132-Genova
Italy
Tel: +390103538259
Fax:+390103538267
Laura.Canesi@unige.it

Published in Chemosphere on 24 July 2017, Volume 186 (2017) 1-9
https://doi.org/10.1016/j.chemosphere.2017.07.120

Abstract

The potential release of nanoparticles (NPs) into aquatic environments represents a growing concern for their possible impact on aquatic organisms. In this light, exposure studies during early life stages, which can be highly sensitive to environmental perturbations, would greatly help identifying potential adverse effects of NPs. Although in the marine bivalve *Mytilus spp.* the effects of different types of NPs have been widely investigated, little is known on the effects of NPs on the developing embryo. In *M. galloprovincialis*, emerging contaminants were shown to affect gene expression profiles during early embryo development (from trocophorae-24 hpf to D-veligers-48 hpf). In this work, the effects of amino-modified polystyrene NPs (PS-NH_2) on mussel embryos were investigated. PS-NH_2 affected the development of normal D-shaped larvae at 48 hpf (EC_{50} = 0.142 mg/L). Higher concentrations (5-20 mg/L) resulted in high embryotoxicity/developmental arrest. At concentrations ≅ EC_{50}, PS-NH_2 affected shell formation, as shown by optical and polarized light microscopy. In these conditions, transcription of 12 genes involved in different biological processes were evaluated. PS-NH_2 induced dysregulation of transcription of genes involved in early shell formation (Chitin synthase, Carbonic anhydrase, Extrapallial Protein) at both 24 and 48 hpf. Decreased mRNA levels for ABC transporter p-glycoprotein-ABCB and Lysozyme were also observed at 48 hpf. SEM observations confirmed developmental toxicity at higher concentrations (5 mg/L). These data underline the sensitivity of *Mytilus* early embryos to PS-NH_2 and support the hypothesis that calcifying larvae of marine species are particularly vulnerable to abiotic stressors, including exposure to selected types of NPs.

Keywords: nanoparticles; amino modified nanopolystyrene; marine mussel; embryo; shell formation; gene transcription.

Running title: Impact of PS-NH_2 on *Mytilus galloprovincialis* early embryo development

1. Introduction

The continuous production and usage of nanoparticles (NPs) will inevitably lead to their environmental release in substantial amounts into water compartments, with potential adverse effects for aquatic organisms (Baker et al., 2014; Corsi et al., 2014). In this light, the utilization of early life stage toxicity tests, involving exposure during the most sensitive stages of the organism to environmental stress, would greatly help in the identification of those NPs that represent a major threat to aquatic species (Paterson, 2011; Zhang et al., 2012; Gambardella et al., 2015). This also applies to studies on the biological impact of NPs on marine invertebrates where, complimentary to the use of adult specimens, embryos have emerged as valid tools for studies on developmental perturbations induced by different types of NPs (Corsi et al., 2014; Canesi and Corsi, 2016). Echinoderms have been so far the most studied taxonomic group of marine invertebrates in assessing NP developmental toxicity (reviewed in Canesi and Corsi, 2016). Several types of NPs (metal based NPs and metal-oxides, carbon based NPs, nanopolymers etc.) resulted in different degrees of embryotoxicity in different sea urchin species at concentrations of μg-mg/L (Canesi and Corsi, 2016). Although these studies demonstrated that in the sea urchin model embryo development can represent a significant target for different types of NPs, in a concentration range of μg/L - low mg/L, information on the underlying molecular mechanisms is still extremely scarce. Only a few data are available in bivalve molluscs: in the oyster *Crassostrea virginica* C_{60} fullerene affected embryonic development from concentrations as low as 10 μg/L (Ringwood et al., 2009, 2010). In contrast, in the mussel *Mytilus galloprovincialis*, metal oxide NPs (n-Fe_2O_3 and n-TiO_2) were ineffective unless at high mg/L concentrations (Kadar et al., 2010; Libralato et al., 2013; Balbi et al., 2014).

Nanoplastics represent an emerging type of NPs of environmental concern. The continuous increase of plastic wastes and debris in the aquatic environment, including estuarine and coastal areas, is increasing the worldwide attention on the possible impact of micro and nano-plastics on marine biota (Moore, 2008; Mattsson et al., 2015; Lambert and Wegner, 2016). Polystyrene (PS) is among

79 the most largely used plastics worldwide, accounting for 24% of the macroplastics in the estuarine
80 habitat, and it can be found in the oceans and in marine organisms as micro- and nano-debris
81 (Browne et al., 2008; Moore, 2008; Andrady 2011; Plastic Europe, 2013). Recent data showed that
82 polystyrene NPs affect embryo development in marine invertebrates: in the sea urchin
83 *Paracentrotus lividus*, amino modified polystyrene NPs (PS-NH_2) caused severe developmental
84 defects at both 24 and 48 hpf. In brine shrimp larvae (*Artemia franciscana*) PS NPs were shown to
85 affect food uptake (feeding), behavior (motility) and physiology (multiple molting) (Bergami et al.,
86 2016). PS-NH_2 has been shown to affect the immune function in *M. galloprovincialis* (Canesi et al.,
87 2015; Canesi et al., 2016); however, no information is available on the possible impact of
88 nanoplastics on embryo development of bivalve species.
89 In *M. galloprovincialis*, changes in gene transcription occurring during early development (from
90 fertilized eggs to 24 hpf and 48 hpf) have been recently investigated. The results underlined the
91 molecular mechanisms involved in the early critical stages, such as the formation of the first shelled
92 embryo, and the adverse effect of estrogenic compounds on transcription of genes related to
93 neuroendocrine signaling and biomineralization (Balbi et al., 2016). In this work, the effects of
94 amino modified polystyrene NPs (PS-NH_2) on mussel embryo development were investigated.
95 Fertilized eggs were exposed to different concentrations of PS-NH_2 (from 0.001 to 20 mg/L) and
96 EC_{50} values were determined in the 48 h embryotoxicity test as previously described (Fabbri et al.,
97 2014). Larval morphology at 48 hpf was also evaluated by polarized light microscopy and scanning
98 electron microscopy (SEM) at different exposure concentrations. The differential expression of
99 selected genes related to known biological functions in adult mussels and whose transcriptional
100 changes are regulated from eggs to 48 hpf in physiological conditions (Balbi et al., 2016) was
101 assessed: these include genes involved in biomineralization, neuroendocrine signaling, immune
102 response, antioxidant defense, biotransformation, autophagy and apoptosis.
103
104 **2. Methods**

105 *2.1 PS-NH_2 characterization*

106 Primary characterization of unlabelled 50 nm amino polystyrene NPs (PS-NH_2), purchased from
107 Bangs Laboratories, was performed as previously described (Della Torre et al., 2014a; Canesi et al.,
108 2015; Canesi et al. 2016; Bergami et al., 2016). PS-NH_2 suspensions (50 µg/ml) were prepared in
109 artificial sea water (ASW) (pH 8, salinity 36‰; ASTM 2004) and filtered with 0.22 µm membrane.
110 Suspensions were quickly vortexed prior to use but not sonicated. Size (Z-average and
111 polydispersity index, PDI) and zeta potential (ζ-potential, mV) were determined by Dynamic Light
112 Scattering (Malvern instruments), using a Zetasizer Nano Series software, version 7.02 (Particular
113 Sciences, UK). Measurements were performed in triplicate, each containing 11 runs of 10 seconds
114 for determining Z-average, 20 runs for the ζ-potential.
115 PS-NH_2 suspensions in ASW (25 µg/mL) were also pelleted by centrifugation and resuspended in
116 MilliQ water, in order to eliminate the excess NaCl, and resuspended in 1 mL of MilliQ water.
117 After vortexing, two drops of the suspension were placed on a lacey carbon holder and left to dry in
118 air without coating. Samples were observed by field emission scanning electron microscopy
119 (FESEM) on a ZeissSUPRA40VP scanning electron microscope operating at 20 kV and by
120 transmission electron microscopy (TEM) (Tecnai G2 Spirit BioTWIN Philips, Eindhoven) The
121 Netherlands). The results on characterization of PS-NH_2 suspensions are summarized in Fig. S1.
122

123 *2.2 Mussels and gamete collection*

124 Sexually mature mussels (*M. galloprovincialis* Lam.), purchased from an aquaculture farm in the
125 Ligurian Sea (La Spezia, Italy) between November and March, were transferred to the laboratory
126 and acclimatized in static tanks containing aerated artificial sea water (ASTM, 2004), pH 7.9-8.1,
127 36 ppt salinity (1 L/animal), at 16 ± 1°C. Mussels were utilized within 2 days for gamete collection.
128 When mussels beginning to spontaneously spawn were observed, each individual was immediately
129 placed in a 250 ml beaker containing 200 ml of aerated ASW until complete gamete emission. After
130 spawning, mussels were removed from beakers and sperms and eggs were sieved through 50 µm

and 100 μm meshes, respectively, to remove impurities. Egg quality (shape, size) and sperm motility were checked using an inverted microscope. Eggs were fertilized with an egg:sperm ratio 1:10 in polystyrene 96-microwell plates (Costar, Corning Incorporate, NY, USA). After 30 min fertilization success (n. fertilized eggs/n. total eggs × 100) was verified by microscopical observation (>85%).

2.3 Embryotoxicity test

The 48-h embryotoxicity assay (ASTM, 2004) was carried out in 96-microwell plates as described by Fabbri et al., (2014). Aliquots of 20 μl of 10x suspensions of PS-NH_2 (obtained from a 20 g/L stock suspension in MilliQ water), suitably diluted in filter sterilized ASW, were added to fertilized eggs in each microwell to reach the nominal final concentrations (0.001-0.01-0.05-0.1-0.25-0.5-1-2.5-5-10-20 mg/L) in a 200 μl volume. At each dilution step, all suspensions were immediately vortexed prior to use. Microplates were gently stirred for 1 min, and then incubated at 18 ± 1°C for 48 h, with a 16h:8 h light:dark photoperiod. All the following procedures were carried out following ASTM 2004. At the end of the incubation time, samples were fixed with buffered formalin (4%). All larvae in each well were examined by optical and/or phase contrast microscopy using an inverted Olympus IX53 microscope (Olympus, Milano, Italy) at 40X, equipped with a CCD UC30 camera and a digital image acquisition software (cellSens Entry). Observations were carried out by an operator blind to the experimental conditions. A larva was considered normal when the shell was D-shaped (straight hinge) and the mantle did not protrude out of the shell, and malformed if had not reached the stage typical for 48 hpf (trocophore or earlier stages) or when some developmental defects were observed (concave, malformed or damaged shell, protruding mantle). The recorded endpoint was the percentage of normal D-larvae (D-veligers) in each well respect to the total, including malformed larvae and pre-D stages. The acceptability of test results was based on controls for a percentage of normal D-shell stage larvae >75% (ASTM, 2004).

In a separate set of experiments, the embryotoxicity test was also carried out by exposing either fertilized eggs or embryos developed at 24 hpf to a single concentration of PS-NH_2 (0.150 mg/L). All other experiments were carried out adding PS-NH_2 to fertilized eggs, unless otherwise indicated. Light microscopy images of D-veligers at 48 h in different experimental conditions were also analyzed for shell length (the anterior-posterior dimension of the shell parallel to the hinge line) and height (the dorsal-ventral dimension perpendicular to the hinge) (Kurihara et al., 2007, 2009).

2.4. Polarized light microscopy and Scanning Electron Microscopy (SEM)

For observations by polarized light microscopy, control embryos and embryos treated with 0.150 mg/L PS-NH_2 grown in 96-microwell plates at 48 hpf were collected by filtration on 0.20 µM filters (about 500 embryos/sample). Each sample was washed four times with deionized water to remove excess salts, and dried at 60°C for 30 min. Observations (40x) were carried out on glass slides by a polarized light microscope (OLYMPUS BX-41). Images were acquired by an Olympus Color view II and digitalized by the Olympus Color view II Bund Cell B.

For SEM observations, control embryos and embryos treated with 5 mg/L PS-NH_2 at 48 hpf were fixed in 3% glutaraldehyde in ASW. After fixation, samples from 6 microwells were pooled, placed onto Whatman 22 µm filters, dehydrated in an ascending series of ethanol washes (50% - 80% - 90% - 100%) and air-dried. Then samples were sputter-coated with gold, and observed at 20 kV with a Vega3 - Tescan scanning electron microscope. All procedures were carried out as previously described (Balbi et al., 2016).

2.5 RNA extraction and qRT-PCR analysis

Unfertilized eggs (about 24,000 eggs/ml) obtained from at least 6 female individuals were collected by centrifugation at 400 xg for 10 min at 4°C, and the resulting pellet was frozen in liquid nitrogen. Eggs were fertilized with an egg:sperm ratio 1:10 in polystyrene 6-well plates and a final 8 ml volume. After 30 min, fertilization success (n. fertilized eggs / n. total eggs x 100) was verified by

182 microscopical observation (>85%). At 30 min pf, PS-NH_2 was added to fertilized eggs in each well
183 from 20 g/L concentrated stock solutions prepared in MilliQ water, immediately vortexed and
184 suitably diluted to reach the final nominal concentration of 0.150 mg/L. Concentration was chosen
185 on the basis of the dose-response curve obtained in the *Mytilus* 48 h embryotoxicity test (present
186 study). Control wells (negative controls) contained only ASW. Four replicates for each
187 experimental condition were made.
188 At 24 and 48 hpf larvae were collected by a nylon mesh (20 μm pore-filter) and washed with ASW.
189 Three wells for each condition were pooled in order to obtain approximately 7000
190 embryos/replicate. The larval suspension was centrifuged at 800 x g for 10 min at 4°C. Larval
191 pellets and unfertilized eggs were lysed in 1 ml of the TRI Reagent (Sigma Aldrich, Milan, Italy)
192 and total RNA was extracted following manufacturer's instructions. RNA concentration and quality
193 were verified using the Qubit RNA assay (Thermo Fisher, Milan, Italy) and electrophoresis using a
194 1.5% agarose gel under denaturing conditions. First strand cDNA for each sample was synthesized
195 from 1 μg total RNA (Balbi et al. , 2014). Gene transcription was evaluated in 4 independent RNA
196 samples.
197 Primers pairs employed for qRT-PCR analysis were as reported in previous studies or were
198 designed with Primer Express (Thermo Fisher, Milan, Italy) using nucleotide sequences retrieved
199 from the GeneBank database (https://www.ncbi.nlm.nih.gov/genbank/) for *Mytilus*
200 *galloprovincialis* (Table S1). qPCR reactions were performed in triplicate in a final volume of 15 μl
201 containing 7.5 μl iTaq universal master mix with ROX (BioRad Laboratories, Milan, Italy), 5 μl
202 diluted cDNA, and 0.3 μM specific primers (Table S1). A control lacking cDNA template (no-
203 template) was included in the qPCR analysis to determine the specificity of target cDNA
204 amplification. Amplifications were performed in a StepOne real time PCR system apparatus
205 (Thermo Fisher, Milan, Italy) using a standard "fast mode" thermal protocol. For each target
206 mRNA, melting curves were utilized to verify the specificity of the amplified products and the
207 absence of artifacts. HEL and EF-α1 were utilized as the best performing combination of reference

gene products (EF1/HEL) for data normalization (Balbi et al., 2016). Calculations of relative expression of target mRNAs was performed by a comparative C_T method (Schmittgen and Livak, 2008) using the StepOne software tool (Thermo Fisher, Milan, Italy). Data were reported as relative expression (fold change or log2-transformed fold changes according to the data ranges) with respect to unfertilized eggs (basal gene expression across larval development) or to control samples within each life stage (PS-NH_2 treatment).

2.6 Data analysis

Embryotoxicity test data were expressed as means ± SDs of 4 experiments carried out in 6 replicate-wells. Data on gene transcription were obtained from 4 independent RNA samples and data expressed as means ± SDs. Statistical differences were evaluated with respect to controls ($P \leq 0.05$, Mann-Whitney U-test). Deviations from parametric test assumptions were verified through the Shapiro-Wilk's test (Normality) and the Bartlett's test (equal variance). The EC_{50} was defined as the concentration of chemical causing 50% reduction in the embryogenesis success, and 95% confidence intervals (CI) were calculated by PRISM 5 software (GraphPad Prism 5 software package, GraphPad Inc).

Gene transcription data were also submitted to permutation multivariate analysis of variance (PERMANOVA) using PRIMER v6 (Anderson et al., 2008). Log-transformed fold changes were used to calculate similarity matrices (Euclidean distance, 999 permutations). Factors considered were "developmental stage" and "PS-NH_2" treatment. Pseudo-F values in the PERMANOVA main tests were evaluated in terms of significance (Anderson et al., 2008). When the main test revealed statistical differences ($P<0.05$), permutation t-tests through PERMANOVA pairwise comparisons were carried out (Euclidean distance matrix, 999 permutations). Distance-based redundancy linear modeling (DISTLM) followed by a redundancy analysis (dbRDA) in PRIMER was also performed to examine the relationship between the multivariate dataset (i.e. the suite of biological endpoints assayed and their variations) and the predictor variables (life stage and PS-NH_2 treatment).

234 Numerical metric for life stage progression was indicated by the post fertilization time (0 h:
235 unfertilized egg; 24 h: trocophorae; 48 h: D-veliger). Treatment was indicated by the nominal
236 concentrations of PS-NH_2 exposure (150 µg/L). DISTLM used the BEST selection procedure and
237 adjusted R^2 selection criteria.
238
239 **3. Results**
240 *3.1 Effects of PS-NH_2 on embryo development*
241 Fertilized eggs were exposed to different concentrations (from 0.001 to 20 mg/L) of PS-NH_2 in 96-
242 microwell plates, and the percentage of normal D-larvae was evaluated after 48 hpf. The results,
243 reported in Fig. 1, show that PS-NH_2 induced a dose-dependent decrease in normal larval
244 development, with an EC_{50} value of 0.142 mg/L (0.09178 - 0.2345 mg/L) (Fig. 1A). The effect was
245 significant from 0.01 mg/L (-34%; $P \leq 0.01$) and was dramatic (-80%) from concentrations ≥ 2.5
246 mg/L. As shown in Fig. 1B, the effect of exposure to PS-NH_2 was biphasic: PS-NH_2 at lower
247 concentrations (from 0.001 to 1 mg/L) mainly induced malformations of the D-veligers. At higher
248 concentrations (from 2.5 mg/L to 10 mg/L), a delay in development was observed, with a
249 progressive increase in the presence of embryos at the pre-veliger stage and a stable proportion of
250 embryos still at the trocophora stage. At the highest concentrations tested (20 mg/L) PS-NH_2
251 completely inhibited the formation of the D-shaped veliger, with about 90% of the larvae withheld
252 at the trocophora stage. In a separate set of experiments, the 48 h embryotoxicity test was carried
253 out adding a single concentration of PS-NH_2 close to the obtained EC_{50} values (0.150 mg/L) to
254 either fertilized eggs or embryos at 24 hpf, when all embryos were developed into the trocophora
255 stage. Although the time of exposure did not significantly affect the percentage of normal D-
256 veligers (i.e. the endpoint of the embryotoxicity test), a higher percentage of immature embryos
257 (pre-veligers and trocophorae) was observed when PS-NH_2 were added to trocophorae with respect
258 to fertilized eggs.
259 All subsequent experiments were carried out adding PS-NH_2 to fertilized eggs as in the standard

embryotoxicity assay. Representative light microscopy images of control embryos and embryos exposed to different concentrations of PS-NH_2 (0.150 - 1 - 2.5 - 5 mg/L) at 48 hpf, showing both malformed and immature embryos, are reported in Fig. S2 (A-D). When the size of D-veligers was evaluated, a small but significant decrease in shell length (-20-30%) was recorded in PS-NH_2-exposed samples, irrespective of the exposure concentration, whereas shell height was unaffected (Fig. S2E).

Fertilized eggs were exposed to PS-NH_2 (at a concentration of 0.150 mg/L, close to the EC_{50} values obtained at 48 hpf) and D-veligers were observed by polarized light microscopy, to evaluate the degree of shell mineralization, based on the observed birefringence due to the mineral phase (Weiss et al. 2002; Kurihara et al. 2007, 2009). Representative images reported in Fig. 2 show that control D-veligers exhibited a rather weak but evident birefrangence over most of the shell area, in particular along the hinge and the margins of the valvae, indicating partial shell mineralization (Fig. 2A and 2B). In contrast, in malformed D-veligers from PS-NH_2 -treated samples birefrangence was almost absent (Fig. 2C and 2D).

3.2 Effects of PS-NH_2 on gene transcription

The effects of exposure of fertilized eggs to PS-NH_2 (0.150 mg/L) on gene transcription was evaluated at different times pf (24 and 48 h). Transcription of 12 selected genes related to neuroendocrine signaling (serotonin receptor, 5-HTR), antioxidant defense (catalase-CAT, superoxide dismutase-SOD), biotransformation (glutathione transferase-GST, ABC transporter p-glycoprotein-ABCB), biomineralization (extrapallial protein, EP, carbonic anhydrase, CA), autophagy, growth and metabolism (serine/threonine-protein kinase mTor), apoptosis (p53), immune response (Toll-like receptor, TLR-i), was evaluated. All these genes, except for GST, were previously shown to be up-regulated across different stages (from eggs to 24 h and 48 hpf) under normal physiological conditions (Balbi et al., 2016). In addition, transcription of chitin synthetase-CS and Lysozyme-LYSO, genes involved in shell formation and immune response/intracellular

digestion, respectively, was evaluated. The results of basal expression of CS and LYSO in untreated embryos are shown in Fig. S3. Data, reported as log2-transformed relative expressions with respect to unfertilized eggs, indicate a slight down-regulation of CS at 24 hpf, followed by a strong up-regulation at 48 hpf. Levels of mRNA for Lysozyme were extremely low at 24 hpf in comparison to eggs; however, a large increase in transcription was observed from 24 to 48 hpf.

The effects of PS-NH_2 exposure on gene expression are shown in Fig. 3. As shown in Fig. 3A, PS-NH_2 induced up-regulation of CS, CA and EP at 24 hpf, in particular of CS (1.7-fold increase with respect to controls; $P \leq 0.05$). In contrast, a general down-regulation of all genes was observed at 48 hpf (about -40%). The effect was significant for both CS and CA (-35% and -50%, respectively; $P \leq 0.05$). A similar trend was observed in transcription of the ABCB gene, with significant up-regulation at 24 hpf (+46%; $P \leq 0.05$) and down-regulation at 48 hpf (-44%; $P \leq 0.05$). PS-NH_2 also induced a significant decrease in mRNA levels for Lysozyme at both times pf (-36 and -46%, respectively, $P \leq 0.05$). No effects were observed in transcription of all the other genes at 24 and 48 hpf. On the whole, results from PERMANOVA and permutation t-test analyses demonstrated that the effects of PS-NH_2 on gene transcription were statistically significant only in the D-veliger stage ($P<0.05$; Table 2S). Indeed, distance-based linear model (DISTLM) analysis revealed that though expression profiles were strongly dependent on embryo development (explaining about 91% total variation, in agreement with Balbi et al., 2016), PS-NH_2 treatment accounted for about 6.3% of total variation, which mostly explained the observed changes in transcript expressions at 48 hpf (Fig. 3B). PERMANOVA analysis also showed a significant interaction between the two factors "developmental stage" and "PS-NH_2" treatment ($P<0.05$; Table S2).

3.3 Scanning Electron Microscopy (SEM)

Control samples and samples exposed to higher concentrations of PS-NH_2 (5 mg/L) at 48 hpf were also observed by SEM as previously described (Balbi et al., 2016), and the results are reported in Fig.4. Fig. 4A shows a representative image of a normal D-veliger, characterized by a shell with

312 straight hinge, symmetric valvae, and uniform surface. In PS-NH_2-treated samples, the results
313 confirm the presence of embryos still at the trocophora stage (Fig. 4B); shelled embryos were
314 represented by malformed D-veligers and preveligers, characterized by externalized velum
315 (arrows) and showing thin valvae with irregular surfaces (Fig. 3C-E). Small preveligers with shells
316 made of thin cracked lamellar structures were also observed (Fig. 4E-F). Malformed embryos
317 covered in small PS-NH_2 agglomerates (Fig. 4G, I). These latter had with a size ranging from 200
318 to 500 nm (Fig. 4H, L). These agglomerates often showed a rough surface, suggesting that they
319 were surrounded by organic material (Fig. 4H).
320
321 **4. Discussion**
322 The results demonstrate that PS-NH_2 significantly affect *M. galloprovincialis* early development in
323 a wide concentration range, with an EC_{50} of 0.142 mg/L. PS-NH_2 showed the first significant
324 effects at concentrations as low as 0.001 mg/L, followed by a dose-dependent increase in the
325 percentage of malformed D-veligers at increasing concentrations, up to 1 mg/L. At higher
326 concentrations, PS-NH_2 induced a progressive delay in development, up to a complete
327 developmental arrest at the highest concentration tested (20 mg/L), where all embryos were
328 withheld at the trocophora stage. Almost identical results were observed in experiments carried out
329 in both 2015/16 and 2016/17 (not shown).
330 Overall, the results indicate a much higher susceptibility of *Mytilus* embryos to PS-NH_2 in
331 comparison with different types of nano-oxides (Kadar et al., 2010; Libralato et al., 2013; Balbi et
332 al., 2014; Canesi, unpublished results). The same PS-NH_2 have been previously shown to induce
333 developmental toxicity in the sea urchin *Paracentrotus lividus*, with EC_{50} values of 3.82 mg/L and
334 2.61 mg/L at 24 and 48 hpf, respectively. In particular, at 48 hpf, PS-NH_2 caused various larval
335 alterations as incomplete or absent skeletal rods, fractured ectoderm, reduced length of the arms and
336 high percentage of blocked embryos (Della Torre et al., 2014a). The EC_{50} obtained in the 48 h

337 mussel embryotoxicity test was one order of magnitude lower than that calculated for the sea
338 urchin, further underlying the sensitivity of *Mytilus* embryos to PS-NH_2.
339 The effects of NPs on marine invertebrates are influenced by their behavior in high ionic strength
340 media (Canesi and Corsi, 2016). Characterization of PS-NH_2 in sea water suspensions indicated that
341 these particles retain a positive surface charge, with ζ potential of +13 and +14 mV in natural and
342 artificial SW, respectively (Della Torre et al., 2014a; Canesi et al., 2015; Canesi et al., 2016;
343 Bergami et al., 2016). In contrast, PS-COOH (ζ potential of -7 mV in NSW) did not show sea
344 urchin embryotoxicity up to concentrations of 50 mg/L (Della Torre et al., 2014a). Similar results
345 were obtained in mussels with metal oxide NPs such as n-TiO_2 (Libralato et al., 2013), that also
346 show negative ζ potentials in ASW (Doyle et al., 2014). Since both anionic and cationic PS NPs and
347 n-TiO_2 showed a comparable degree of agglomeration in marine water at concentrations between
348 0.1 and 1 mg/L (with the formation of stable agglomerates of about 200 nm in size) (Canesi et al.,
349 2014; Della Torre et al. 2014a), the results suggest that the positive surface charge retained in sea
350 water, rather than core composition or differences in agglomeration state, may play a key role in
351 determining the developmental effects of different types of NPs in marine invertebrates. Overall,
352 these data confirm that in marine organisms, like in mammalian systems, cationic NPs are
353 generally more toxic with respect to anionic ones (Bexiga et al., 2011).
354 The cumulative effects of PS-NH_2 on mussel embryo development were apparently independent on
355 the timing of exposure. When in a separate set of experiments PS-NH_2 was added either to
356 fertilized eggs or to embryos at 24 hpf, at a concentration close to the EC_{50} (0.150 mg/L), no
357 significant differences in the percentage of normal D-veligers were observed at 48 hpf. However,
358 exposure at 24 hpf induced a higher proportion of immature larvae, suggesting that the processes
359 involved in the transition from the trocophora stage (24 hpf) to the first shelled embryo of D-veliger
360 (48 hpf) were mostly affected.
361 In order to gain an insight on the possible effects of PS-NH_2 (0.150 mg/L) on shell formation, the
362 degree of mineralization of mussel embryos at 48 hpf was estimated by polarized light microscopy.

On the basis of the observed shell birefringence, which is due to the mineral phase, the larval area exhibiting birefringence can be interpreted to be covered by mineralized shell (Weiss et al., 2002). Bivalve larvae, including mussels, initially deposit amorphous calcium carbonate (ACC) in the shell (Weiss, 2002; Balbi et al., 2016), that is then partially transformed to aragonite, in contrast to adult shells that are predominantly composed of calcite. According to Weiss (2002), bivalve larvae can be categorized into 3 types; fully mineralized (individuals that exhibit birefringence over the entire surface of the larva), partially mineralized (individuals in which only part of the larval surface exhibits birefringence), and non-mineralized (larvae that exhibit no birefringence). Our data show a visible birefringence in control embryos, indicating the presence of a partially mineralized shell. In samples exposed to PS-NH_2, no birefringence was observed. Since at 48 hpf the birefringence signal was weak also in control D-veligers, as previously observed in oyster embryos at the same time pf (Kurihara et al., 2007, 2009), its absence in PS-NH_2 -treated samples does not indicate that the shell only consisted of ACC, but suggests that exposure to PS-NH_2 may affect the crystallization process.

The possible mechanisms underlying the effects of PS-NH_2, in the same experimental conditions, were investigated by evaluating transcription of selected genes by qRT-PCR. We have recently shown that in *M. galloprovincialis* significant increases in basal transcription of a number of genes involved in neuroendocrine signaling, biomineralization, immune and antioxidant defense occur across early developmental stages (eggs, 24 hpf, 48 hpf) (Balbi et al., 2016). In particular, the results underlined the role of genes involved in the initial formation of a first calcified shell (prodissoconch I), such as carbonic anhydrase (CA), that regulates matrix mineralization by generating an acidic environment (Clark et al., 2010) and *Mytilus* EP (Extrapallial Protein), an acidic calcium binding protein that regulates the production of different polymorphs of calcium carbonate (Yin et al., 2009). In basal conditions, both EP and CA showed highest expression at 48 hpf, confirming the key physiological role of both transcripts in initial biomineralization (Balbi et al., 2016). In this work, transcription of Chitin synthase (CS) was also evaluated. CSs are

389 transmembrane glycosyltransferases that are responsible for the enzymatic synthesis of chitin, that
390 not only represents a key structural component of the shell matrix, but also forms the framework for
391 other macromolecules that guide initial shell deposition (Schönitzer and Weiss, 2007; Weiss and
392 Schönitzer. 2006). Despite the importance of chitin synthesis in the formation of bivalve shells
393 (Weiss et al., 2006), no information is available on expression of chitin synthase during early
394 embryo stages. The results here obtained show that in control samples the level of transcripts for CS
395 was slightly lower at 24 hpf with respect to the eggs, indicating that at this stage embryos still rely
396 on maternal mRNA for this gene; however, a large increase in transcription of CS was recorded
397 from 24 to 48 hpf, confirming the key role for chitin synthesis in the formation of the first shell.
398 In samples exposed to PS-NH_2, changes in transcription of CS, CA and EP were observed.
399 Although a general transient up-regulation was observed at 24 hpf, all genes were downregulated at
400 48 hpf. CS was the most affected gene, with significant changes at both times pf and, in particular,
401 at 48 hpf, when the amount of mRNA was reduced by 50% with respect to controls, indicating
402 impairment of the physiological production of chitin. In the same conditions, down-regulation of
403 CA and EP also indicate alterations in $CaCO_3$ deposition and mineralization.
404 Interestingly, PS-NH_2 exposure also modulated expression of an *ABCB* transcript encoding the p-
405 glycoprotein transporter (P-gp), with significant *ABCB* up-regulation and down-regulation at 24 and
406 48 hpf, respectively. The Multi xenobiotic resistance (MXR) system is considered a general and
407 broad spectrum protective mechanism that consists of membrane and intracellular transporters
408 acting as an active first-tier defense against environmental chemicals, preventing their accumulation
409 and toxic effects (Bielen et al., 2016). Among MXR-related proteins in mussels, P-gp is the best
410 characterized in an environmental context. P-gp is a membrane protein that mediates the direct
411 extrusion of un-metabolized xenobiotic out of the cell (i.e. phase 0 transporter) (Bard, 2000;
412 Franzellitti and Fabbri, 2006). In adult mussels, induction of P-gp has been reported in response to a
413 wide range of chemical and physical stressors, suggesting that this transporter may be part of the
414 general cellular stress response machinery. A recent study on expression and activity of MXR

415 across *Mytilus* early development supported the hypothesis that in both embryos and adult mussels
416 P-gp aids in xenobiotic efflux performing a prominent protective role against toxicants (Franzellitti
417 et al., 2016). In particular, increased expression of *ABCB* and appearance of P-gp mediated
418 functional activity were detected at 48 hpf. The results of the present work suggest that exposure to
419 PS-NH_2 may impair the phase 0 of biotransformation of xenobiotics in D-veligers. To our
420 knowledge, this is the first report on the effects of NPs on expression of P-gp transporters in a
421 marine invertebrate embryo. In the sea urchin, much higher concentrations of PS-NH_2 (3 mg/L) did
422 not affect expression of *ABCB* transporters, but induced significant increase in transcription of the
423 cas-8 gene at 24 hpf, suggesting the activation of apoptotic processes (Della Torre et al., 2014b).
424 With regards to genes involved in the immune response, their transcription in bivalve development
425 is generally low at early stages, and increases in later pre-metamorphic stages, when larvae
426 synthesize their own mRNA and proteins, acquiring immunocompetence (Balseiro et al., 2013;
427 Song et al., 2016). Among these, Lysozymes are conserved enzymes that share the ability to split a
428 (1,4) linkage between two amino sugars, N-acetylmuramic acid and N-acetylglucosamine, of the
429 bacterial peptidoglycan. In suspension feeding bivalves, where bacteria also represent a source of
430 food that is processed by intracellular digestion in the hepatopancreas, a molecular evolution of
431 Lysozyme from a defense to a digestive function has been postulated, similar to that observed in
432 mammalian systems (Jollès et al., 1996). In adult *M. galloprovincialis* Lysozyme is expressed not
433 only in immune cells, but also in the hepatopancreas and other tissues (Wang et al., 2012; Balbi et
434 al., 2014). Our data show that in control embryos levels of mRNA for lysozyme were extremely
435 low at 24 hpf in comparison to eggs; however, a large increase in transcription was observed from
436 24 to 48 hpf. Exposure to PS-NH_2 induced significant decreases in transcription of lysozyme at both
437 times pf, indicating interference with the initial progression not only of immunocompetence, but
438 also of processes related to the digestive function.
439 Interestingly, PS-NH_2 did not affect transcription of a number of other genes involved in different
440 key biological functions; in particular, no changes were observed in mRNA levels for the serotonin

441 receptor 5-HTR and antioxidant enzymes, catalase and superoxide dismutase, whose expression in
442 early embryos was previously shown to be modulated by estrogenic compounds (Balbi et al., 2016).
443 This lack of effects further underlines how, in *Mytilus* embryos, exposure to PS-NH_2, at
444 concentrations as low as 0.150 mg/L, specifically affected transcription of genes involved in shell
445 formation, of *ABCB* transporters and lysozyme.
446 The effects of higher concentrations of PS-NH_2 (5 mg/L) on larval morphology was also
447 investigated by SEM as previously described (Balbi et al., 2016). The results confirm the presence
448 of embryos blocked at the trocophora stage and malformed pre-veligers, many of which had a shell
449 made of thin cracked layers of mineralized lamellae, indicating that the process of shell formation
450 was heavily affected in multiple ways depending on the concentration. Overall, the results confirm
451 the biphasic effect PS-NH_2 on embryo development at 48 hpf. Lower concentrations mainly
452 induced shell malformations and affected crystallization of $CaCO_3$, whereas higher concentrations
453 induced developmental arrest and high embryotoxicity. PS-NH_2 internalization by mussel embryos
454 could not be evaluated in the present study. Attempts were made using the same fluorescently
455 labelled (358 nm excitation, 410 nm emission) PS-NH_2 used in the sea urchin study (Della Torre et
456 al., 2014): although a weak and diffuse fluorescence could be observed in samples exposed to 5
457 mg/L (not shown), it was impossible to distinguish internalized particles due to the low florescence
458 signal, as previously shown with the sea urchin embryo (Della Torre et al., 2014).
459 The results of the present work represent the first indication on the molecular mechanisms involved
460 in the possible developmental impact of NPs on bivalve molluscs. Overall, the obtained data
461 underline that the transition from the trocophora stage (24 hpf) to the first shelled embryo D-veliger
462 (48 hpf) represents a critical stage for the effects of PS-NH_2. In particular, the results demonstrate
463 that exposure to PS-NH_2, at concentrations of 0.150 mg/L, resulted in D-veligers showing 50%
464 malformations, reduced shell mineralization and smaller size. Although a number of genes involved
465 in biomineralization are being described in different bivalve species (Bassim et al., 2015; Vendrami
466 et al., 2016), little information is available on those involved in the formation of a first calcified

shell (prodissoconch I), a key step in early development. Our data demonstrate that the effects on PS-NH_2 on D-veligers were associated with down-regulation of genes involved in the early processes of shell formation (i.e. chitin synthesis and $CaCO_3$ deposition). Interestingly, the effects of PS-NH_2 were similar to those observed by exposure to high pCO_2 or low pH (Kadar et al., 2010; Kurihara et al., 2009), as well by pharmacological inhibition of chitin synthesis (Schönitzer and Weiss, 2007; Weiss and Schönitzer, 2006). Calcifying larvae of marine species are particularly vulnerable to abiotic stressors (Przelawski et al., 2015). Our data further support the hypothesis that in *Mytilus* the transition from the trocophora stage to the first D-shelled larva represents a most sensitive step to the action of contaminants (Balbi et al., 2016). In a global change scenario, concomitant changes in environmental parameters (i.e. acidification) and exposure to emerging contaminants such as NPs may represent a serious cause of concern for early life stages of sensitive marine species.

References

Anderson, M., Gorley, R., Clarke, K., 2008. PERMANOVAþ for Primer: Guide to Software and Statistical Methods.

Andrady, A.L., 2011. Microplastics in the marine environment. Mar. Pollut. Bull. 62, 1596-1605.

ASTM, 2004. Standard guide for conducting static acute toxicity tests starting with embryos of four species of saltwater bivalve molluscs. http://dx.doi.org/10.1520/E0724-98.

Baker, T.J., Tyler, C.R., Galloway, T.S., 2014. Impacts of metal and metal oxide nanoparticles on marine organisms. Environ. Pollut. 186, 257-271.

Balbi, T., Franzellitti, S., Fabbri, R., Montagna, M., Fabbri, E., Canesi, L., 2016. Impact of bisphenol A (BPA) on early embryo development in the marine mussel *Mytilus galloprovincialis*: Effects on gene transcription. Environ. Pollut. 218, 996-1004.

Balbi, T., Smerilli, A., Fabbri, R., Ciacci, C., Montagna, M., Grasselli, E., Brunelli, A., Pojana, G., Marcomini, A., Gallo, G., Canesi, L., 2014. Co-exposure to n-TiO_2 and Cd^{2+} results in

493 interactive effects on biomarker responses but not in increased toxicity in the marine bivalve
494 *M. galloprovincialis*. Sci. Total Environ. 493, 355-364.
495 Balseiro, P., Moreira, R., Chamorro, R., Figueras, A., Novoa, B., 2013. Immune responses during
496 the larval stages of Mytilus galloprovincialis: Metamorphosis alters immunocompetence,
497 body shape and behavior. Fish and Shellfish Immun. 3, 438-447.
498 Bard, S.M., 2000. Multixenobiotic resistance as a cellular defense mechanism in aquatic organisms.
499 Aquat. Toxicol. 48, 357-389.
500 Bassim, S., Chapman, R.W., Tanguy, A., Moraga, D., Tremblay, R., 2015. Predicting growth and
501 mortality of bivalve larvae using gene expression and supervised machine learning. Comp.
502 Biochem. Physiol. D 16, 59-72.
503 Bergami, E., Bocci, E., Vannuccini, M.L., Monopoli, M., Salvati, A., Dawson, K.A., Corsi, I.,
504 2016. Nano-sized polystyrene affects feeding, behavior and physiology of brine shrimp
505 *Artemia franciscana* larvae. Ecotoxicol. Environ. Saf. 123, 18-25.
506 Bexiga, M.G., Varela, J.A.,Wang, F., Fenaroli, F., Salvati, A., Lynch, I., Simpson, J.C., Dawson,
507 K.A., 2011. Cationic nanoparticles induce caspase 3-, 7- and 9-mediated cytotoxicity in a
508 human astrocytoma cell line. Nanotoxicology 5, 557-567.
509 Bielen, A., Bošnjak, I., Sepčić, K., Jaklič, M., Cvitanić, M., Lušić, J., Lajtner, J., Simčič, T.,
510 Hudina, S., 2016. Differences in tolerance to anthropogenic stress between invasive and
511 native bivalves. Sci. Total Environ. 543, 449-459.
512 Browne, M.A., Dissanayake, A., Galloway, T.S., Lowe, D.M., Thompson, R.C., 2008. Ingested
513 microscopic plastic translocates to the circulatory system of the mussel, *Mytilus edulis* (L.).
514 Environ. Sci. Technol. 42, 5026-5031.
515 Canesi, L., Ciacci, C., Bergami, E., Monopoli, M.P., Dawson, K.A., Papa, S., Canonico, B., Corsi,
516 I., 2015. Evidence for immunomodulation and apoptotic processes induced by cationic
517 polystyrene nanoparticles in the hemocytes of the marine bivalve *Mytilus*. Mar. Environ.
518 Res. 111, 34-40.

519 Canesi, L., Ciacci, C., Fabbri, R., Balbi, T., Salis, A., Damonte, G., Cortese, K., Caratto, V.,
520 Monopoli, M.P., Dawson, K., Bergami, E., Corsi, I., 2016. Interactions of cationic
521 polystyrene nanoparticles with marine bivalve hemocytes in a physiological environment:
522 Role of soluble hemolymph proteins. Environ. Res. 150, 73-81.
523 Canesi, L., Corsi, I., 2016. Effects of nanomaterials on marine invertebrates. Sci. Total Environ.
524 565, 933-940.
525 Canesi, L., Frenzilli, G., Balbi, T., Bernardeschi, M., Ciacci, C., Corsolini, S., Della Torre, C.,
526 Fabbri, R., Faleri, C., Focardi, S., Guidi, P., Kočan, A., Marcomini, A., Mariottini, M.,
527 Nigro, M., Pozo-Gallardo, K., Rocco, L., Scarcelli, V., Smerilli, A., Corsi, I., 2014.
528 Interactive effects of n-TiO_2 and 2,3,7,8-TCDD on the marine bivalve *Mytilus*
529 *galloprovincialis*. Aquat. Toxicol. 153, 53-65.
530 Clark, M.S., Thorne, M.A., Vieira, F.A., Cardoso, J.C., Power, D.M., Peck, L.S., 2010. Insights into
531 shell deposition in the Antarctic bivalve *Laternula elliptica*: gene discovery in the mantle
532 transcriptome using 454 pyrosequencing. BMC Genomics 11, 362.
533 Corsi, I., Cherr, G.N., Lenihan, H.S., Labille, J., Hassellov, M., Canesi, L., Dondero, F., Frenzilli,
534 G., Hristozov, D., Puntes, V., Della Torre, C., Pinsino, A., Libralato, G., Marcomini, A.,
535 Sabbioni, E., Matranga, V., 2014. Common strategies and technologies for the ecosafety
536 assessment and design of nanomaterials entering the marine environment. ACS Nano 8,
537 9694-9709.
538 Della Torre, C., Bergami, E., Salvati, A., Faleri, C., Cirino, P., Dawson, K.A., Corsi, I., 2014a.
539 Accumulation and embryotoxicity of polystyrene nanoparticles at early stage of
540 development of sea urchin embryos *Paracentrotus lividus*. Environ. Sci. Technol. 48,
541 12302-12311.
542 Della Torre, C., Bocci, E., Focardi, S.E., Corsi, I., 2014b. Differential ABCB and ABCC gene
543 expression and efflux activities in gills and hemocytes of *Mytilus galloprovincialis* and their
544 involvement in cadmium response. Mar. Environ. Res. 93, 56-63.

545 Doyle, J.J., Palumbo, V., Huey B.D., Ward, J.E., 2014. Behavior of titanium dioxide nanoparticles
546 in three aqueous media samples: Agglomeration and implications for benthic deposition,
547 Water Air Soil Poll. 225, 2106-2119.
548 Fabbri, R., Montagna, M., Balbi, T., Raffo, E., Palumbo, F., Canesi, L., 2014. Adaptation of the
549 bivalve embryotoxicity assay for the high throughput screening of emerging contaminants in
550 *Mytilus galloprovincialis*. Mar. Environ. Res. 99, 1-8.
551 Franzellitti, S., Fabbri, E., 2006. Cytoprotective responses in the Mediterranean mussel exposed to
552 Hg^{2+} and CH_3Hg^+. Biochem. Biophys. Res. Commun. 351, 719-725.
553 Franzellitti, S., Striano, T., Pretolani, F., Fabbri, E., 2016. Investigating appearance and regulation
554 of the MXR phenotype in early embryo stages of the Mediterranean mussel (*Mytilus*
555 *galloprovincialis*) Comp. Biochem. Phys. C. http://dx.doi.org/10.1016/j.cbpc.2016.11.004
556 Gambardella, C., Morgana, S., Bari, G.D., Ramoino, P., Bramini, M., Diaspro, A., Falugi, C.,
557 Faimali, M., 2015. Multidisciplinary screening of toxicity induced by silica nanoparticles
558 during sea urchin development. Chemosphere 139, 486-495.
559 Jollès, J., Fiala-Médioni, A., Jollès, P., 1996. The ruminant digestion model using bacteria already
560 employed early in evolution by symbiotic molluscs. J. Mol. Evol. 43, 523-527.
561 Kadar, E., Simmance, F., Martin, O., Voulvoulis, N., Widdicombe, S., Mitov, S., Lead, J.R.,
562 Readman, J.W., 2010. The influence of engineered Fe_2O_3 nanoparticles and soluble ($FeCl_3$)
563 iron on the developmental toxicity caused by CO_2-induced seawater acidification. Environ.
564 Pollut. 158, 3490-3497.
565 Kurihara, H., Asai, T., Kato, S., Ishimatsu, A., 2009. Effects of elevated pCO_2 on early
566 development in the mussel *Mytilus galloprovincialis*. Aquat. Biol. 4, 225-233.
567 Kurihara, H., Kato, S., Ishimatsu, A., 2007. Effects of increased seawater pCO_2 on early
568 development of the oyster *Crassostrea gigas*. Aquat. Biol. 1, 91-98.
569 Lambert, S., Wagner, M., 2016. Formation of microscopic particles during the degradation of
570 different polymers. Chemosphere 161, 510-517.

571 Libralato, G., Minetto, D., Totaro, S., Mičetić, I., Pigozzo, A., Sabbioni, E., Marcomini, A., Volpi
572 Ghirardini, A., 2013. Embryotoxicity of TiO_2 nanoparticles to *Mytilus galloprovincialis*
573 (Lmk). Mar. Environ. Res. 92, 71-78.
574 Mattsson, K., Hansson, L.A., Cedervall, T., 2015. Nano-plastics in the aquatic environment.
575 Environ. Sci. Process Impacts 17, 1712-1721.
576 Moore, C.J., 2008. Synthetic polymers in the marine environment: A rapidly increasing, long-term
577 threat. Environ. Res. 108, 131-139.
578 Paterson, G., Ataria, J.M., Hoque, M.E., Burns, D.C., Metcalfe, C.D., 2011. The toxicity of titanium
579 dioxide nanopowder to early life stages of the Japanese medaka (*Oryzias latipes*).
580 Chemosphere 82, 1002-1009.
581 Plastics Europe, 2013. Plastics - the Facts 2013: An analysis of European latest plastics production,
582 demand and waste data. http://www.plasticseurope.org/Document/plastics-the-facts-
583 2013.aspx.
584 Przeslawski, R., Byrne, M., Mellin, C., 2015. A review and meta-analysis of the effects of multiple
585 abiotic stressors on marine embryos and larvae. Glob. Chang. Biol. 21, 2122-2140.
586 Ringwood, A.H., Levi-Polyachenko, N., Carroll, D.L., 2009. Fullerene exposures with
587 oysters: embryonic, adult, and cellular responses. Environ. Sci. Technol. 43, 7136-7141.
588 Ringwood, A.H., Levi-Polyachenko, N., Carroll, D.L., 2009. Fullerene exposures with oysters:
589 embryonic, adult, and cellular responses. Environ. Sci. Technol. 43, 7136-7141.
590 Ringwood, A.H., McCarthy, M., Bates, T.C., Carroll, D.L., 2010. The effects of silver nanoparticles
591 on oyster embryos. Mar. Environ. Res. 69, 49-51.
592 Schmittgen, T.D., Livak, K.J., 2008. Analyzing real-time PCR data by the comparative C_T method.
593 Nat. Protoc. 3, 1101-1108.
594 Schönitzer, V., Weiss, I.M., 2007. The structure of mollusc larval shells formed in the presence of
595 the chitin synthase inhibitor Nikkomycin Z. BMC Struct. Biol. 7, 71.

596 Song, X., Wang, H., Xin, L., Xu, J., Jia, Z., Wang, L., Song, L., 2016. The immunological capacity
597 in the larvae of Pacific oyster *Crassostrea gigas*. Fish and Shellfish Immun. 49, 461-469.
598 Vendrami, D.L.J., Shah, A., Telesca, L., Hoffman, J.I., 2016. Mining the transcriptomes of four
599 commercially important shellfish species for single nucleotide polymorphisms within
600 biomineralization genes. Mar. Genom. 27, 17-23.
601 Wang, Q., Zhang, L., Zhao, J., You, L., Wu, H., 2012. Two goose-type lysozymes in *Mytilus*
602 *galloprovincialis*: Possible function diversification and adaptive evolution. PLoS One. 7,
603 e45148.
604 Weiss, I.M., Schönitzer, V., 2006. The distribution of chitin in larval shells of the bivalve mollusk
605 *Mytilus galloprovincialis*. J. Struct. Biol. 153, 264-277.
606 Weiss, I.M., Schönitzer, V., Eichner, N., Sumper, M., 2006. The chitin synthase involved in marine
607 bivalve mollusk shell formation contains a myosin domain. FEBS Lett. 580, 1846-1852.
608 Weiss, I.M., Tuross, N., Addadi, L., Weiner, S., 2002. Mollusc larval shell formation: Amorphous
609 calcium carbonate is a precursor phase for aragonite. J. Exp. Zool. 293, 478-491.
610 Yin, H., Ji, B., Dobson, P.S., Mosbahi, K., Glidle, A., Gadegaard, N., Freer, A., Cooper, J.M.,
611 Cusack, M., 2009. Screening of biomineralization using microfluidics. Anal. Chem. 81, 473-
612 478.
613 Zhang, W., Lin, K., Sun, X., Dong, Q., Huang, C., Wang, H., Guo, M., Cui, X., 2012. Toxicological
614 effect of MPA-CdSe QDs exposure on zebrafish embryo and larvae. Chemosphere 89, 52-
615 59.
616
617
618 **Acknowledgements**
619 The Authors thank Laura Negretti for her technical assistance in SEM analyses. This work was
620 partly supported by FRA (Fondi di Ricerca di Ateneo) of the Genoa University.
621

622 **Figure legends**

623 **Fig. 1 - Effects of different concentrations of PS-NH_2 (0.001-0.01-0.05-0.1-0.25-0.5-1-2.5-5-10-**
624 **20 mg/L) on *M. galloprovincialis* normal larval development in the 48 h embryotoxicity assay**.
625 A and B show the results obtained by exposure of fertilized eggs to PS-NH_2. A) Percentage of
626 normal D-shaped larvae with respect to controls. B) Percentage of normal D-veliger (dark grey),
627 malformed D-veliger (light grey) and pre-veligers (white) and trocophorae in each experimental
628 condition. C) same as in B, but showing the effects of addition of a single concentration of PS-NH_2
629 (0.150 mg/L) to either fertilized eggs or at 24 hpf. Data represent the mean ± SD of 4 experiments
630 carried out in 96-multiwell plates (6 replicate wells for each sample).
631
632 **Fig. 2 - Effects of exposure of fertilized eggs to PS-NH_2 (0.150 mg/L) on *Mytilus* embryos at 48**
633 **hpf observed by polarized light microscopy.** Left panels: light microscopy. Right panels:
634 polarized light microscopy. A, B) control embryos, showing weak but evident shell birefringence
635 consistent with a fraction of crystalline shell material (Prodissoconch I); C, D) embryos exposed to
636 0.150 mg/L PS-NH_2, where no birefringence could be observed, indicating the prevalence of
637 amorphous calcium carbonate (ACC) in the shell.
638
639 **Fig. 3 - Effects of exposure of fertilized eggs to PS-NH_2 (0.150 mg/L) on gene transcription in**
640 ***Mytilus* embryos at 24 and 48 hpf.**
641 A) Relative expression of CS (chitin synthetase), CA (carbonic anhydrase), EP (Extrapallial
642 Protein), 5-HTR (5-hydroxyl triptamine receptor), CAT (catalase), Superoxide dismutase (SOD),
643 GST (glutathione transferase), ABCB (ABC transporter p-glycoprotein), mTor (mammalian target
644 of rapamycin), p53, TLR i (Toll-like receptor i isoform), LYSO (Lysozyme). Data are reported as
645 mean ± SD of the relative expression with respect to untreated samples within each life stage (N =
646 4). * $P<0.05$, (Mann-Whitney U test). Further statistical differences were evaluated between
647 trocophorae and D-veligers (# $P<0.05$).

B) Distance-based redundancy (DISTLM) modeling with distance-based redundancy analysis (dbRDA) to explore the amount of the variation in gene transcription to be attributed to PS-NH_2 treatment (150 µg/L) of *Mytilus* embryos at different developmental stages (Euclidean Distance resemblance matrix, 999 permutations).

Fig. 4 - Effects of exposure of fertilized eggs to higher concentrations of PS-NH_2 (5 mg/L) on the morphology of *Mytilus* embryos at 48 hpf evaluated by Scanning electron microscopy (SEM).

A) control D-veliger at 48 hpf, with straight hinge, symmetric valvae and uniform surface.

B-L) representative images of the different effects of PS-NH_2. B: embryo witheld at the trocophora stage; C,E; pre-veligers; D: malformed veliger. Note the present of thin, semi-transparent valvae with irregular shell surfaces. E, F: small malformed shells made of thin cracked lamellae. G,I: malformed embryo and D-shell of a dead embryo covered in small PS-NH_2 agglomerates with a rough (H) or a smooth surface (L). Arrows indicate the presence of externalized velum characteristic of pre-veligers.

Legend to Supplementary Figures

Fig. S1 - Characterization of PS-NH_2 suspensions in different exposure media (from Della Torre et al., 2014; Canesi et al., 2015, 2016).

A) DLS analysis of PS-NH_2 suspensions (50 mg/L) in different media, showing Z-average (nm), polydispersity index (PDI) and ζ-potential (mV). Data are reported as mean ± SD. MQ: Milli-Q water; ASW: artificial seawater. B and C) Representative FESEM and TEM images of PS-NH_2 suspensions in ASW (20 mg/L).

Fig. S2 - Effects of PS-NH_2 of the morphology of *M. galloprovincialis* embryos at 48 hpf.

A-D: representative light microscopy images of control embryos and embryos exposed to different concentrations (1-2.5-5 mg/L) of PS-NH_2. A) Control D-veligers; B) 1 mg/L: malformed D-veligers; C) 2.5 mg/L: pre-veligers; D) 5 mg/L: a malformed D-veliger and a trocophora.

E: effects of different concentrations of PS-NH_2 (0.150 - 1- 2.5- 5 mg/L) on shell growth. D-shaped larvae were measured for shell length (anterior to posterior dimension of the shell parallel to the hinge line) and height (dorsal to ventral dimension perpendicular to the hinge). Significant differences with respect to controls were evaluated by the Mann-Whitney U test (* $P<0.05$).

Fig. 3S - Transcriptional profiles of Chitin synthase (CS) and Lysozyme (LYSO) during early embryo development. Gene transcription was evaluated by qPCR in embryos of *M. galloprovincialis* grown under physiological conditions at 24 (trocophora) and 48 (D-veliger) hpf. Data, reported as log2-transformed relative expressions with respect to unfertilized eggs, represent the mean ± SD (N = 6). Significant differences among different stages were evaluated by 1-way non-parametric ANOVA followed by the Mann-Whitney U test ($P<0.05$).

* trocophora *vs* eggs; ** veliger *vs* eggs; # veliger *vs* trocophora.

Fig. 1

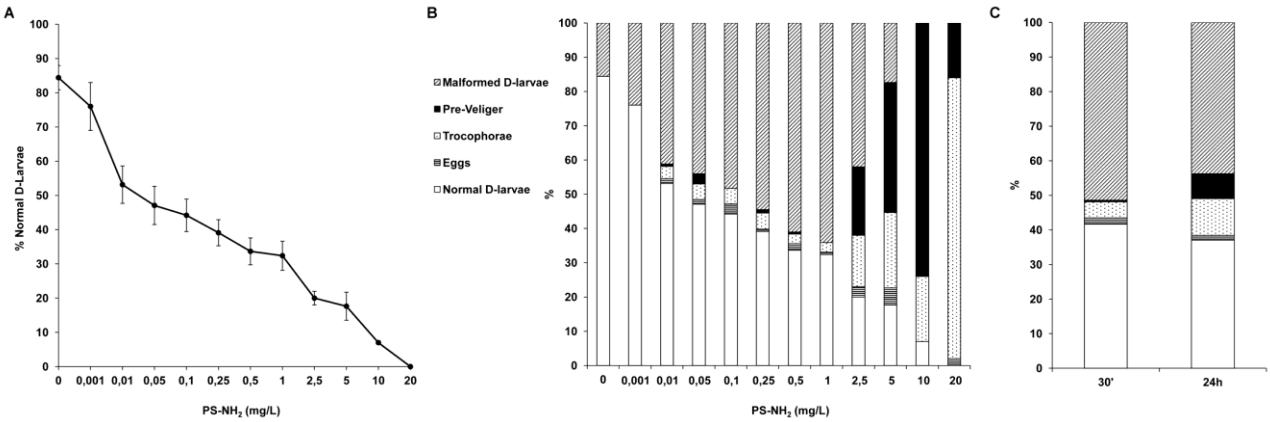
A
% Normal D-Larvae
PS-NH2 (mg/L)
B
Malformed D-larvae
Pre-Veliger
Trocophorae
Eggs
Normal D-larvae
%
PS-NH2 (mg/L)
C
%
30'
24h

Fig. 2

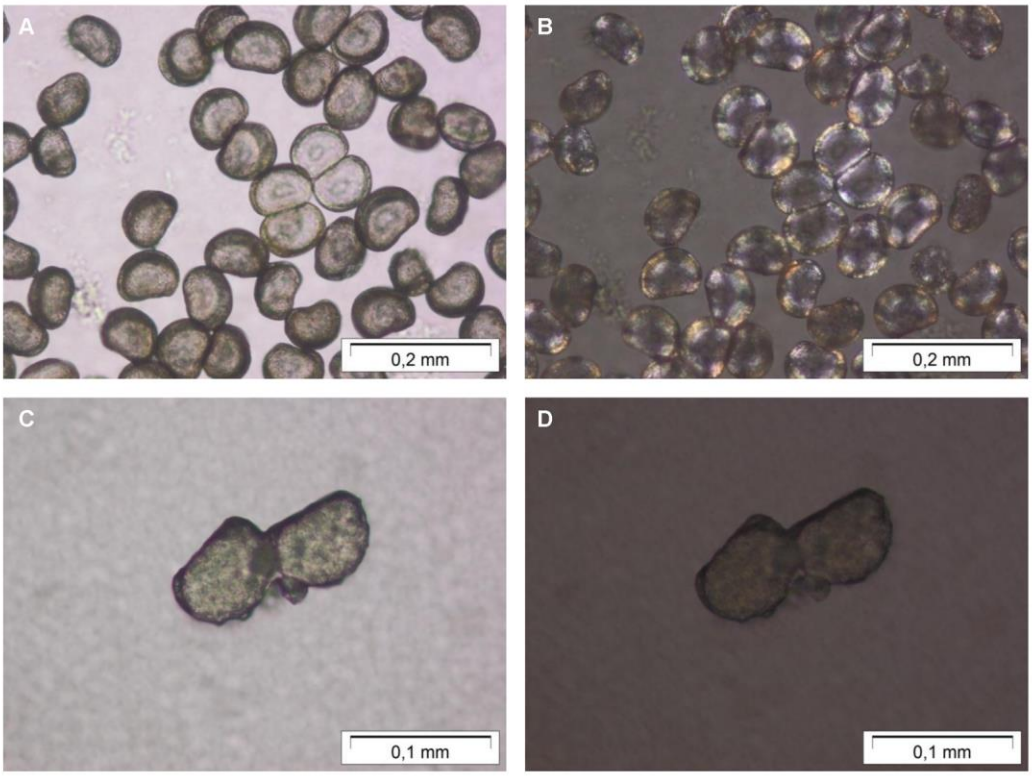

Fig. 3

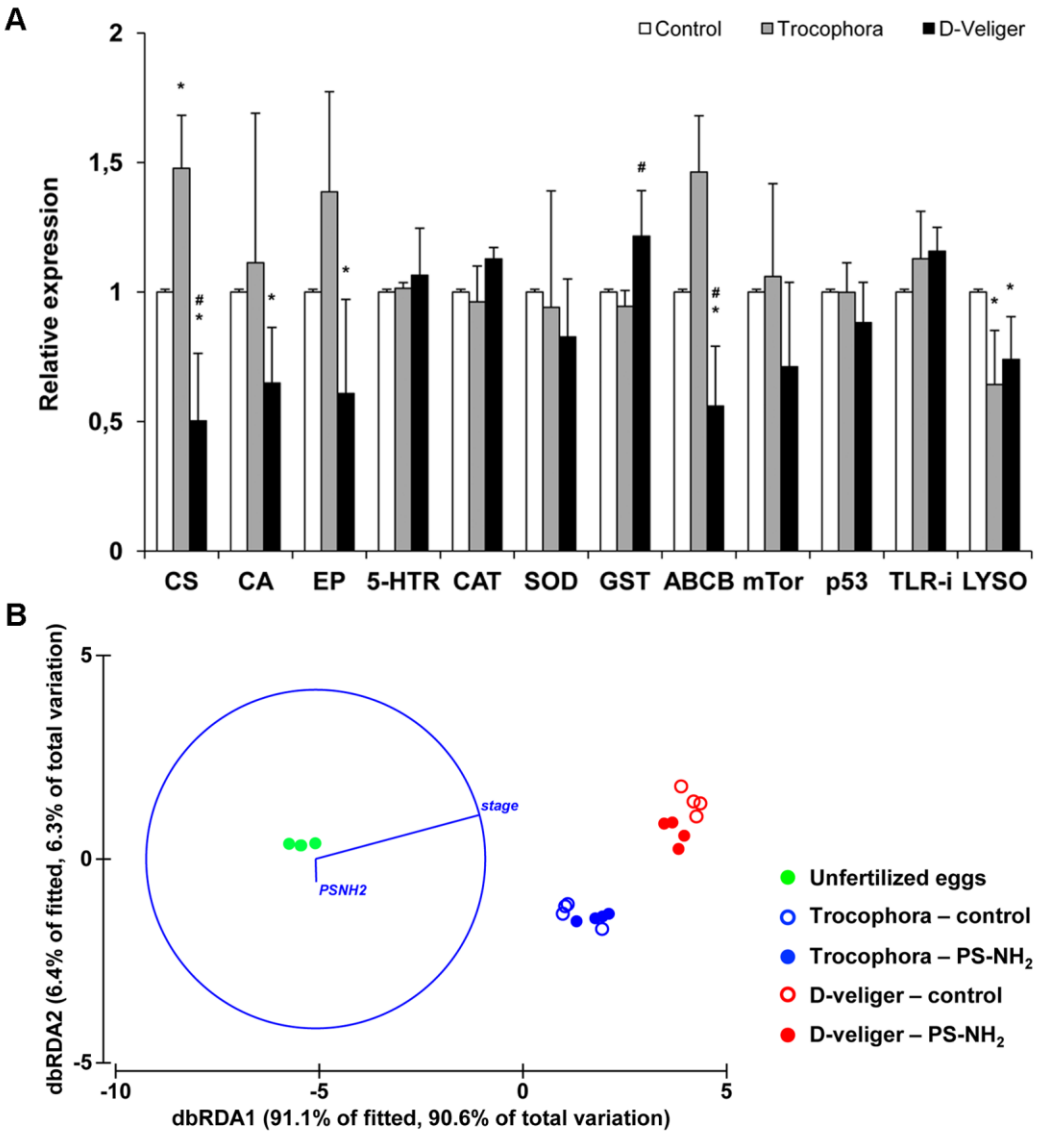
A
Control
Trocophora
D-Veliger
Relative expression
2
1,5
1
0,5
0
CS
CA
EP
5-HTR
CAT
SOD
GST
ABCB
mTor
p53
TLR-i
LYSO
B
dbRDA2 (6.4% of fitted, 6.3% of total variation)
dbRDA1 (91.1% of fitted, 90.6% of total variation)
stage
PSNH2
Unfertilized eggs
Trocophora – control
Trocophora – PS-NH2
D-veliger – control
D-veliger – PS-NH2

Fig. 4

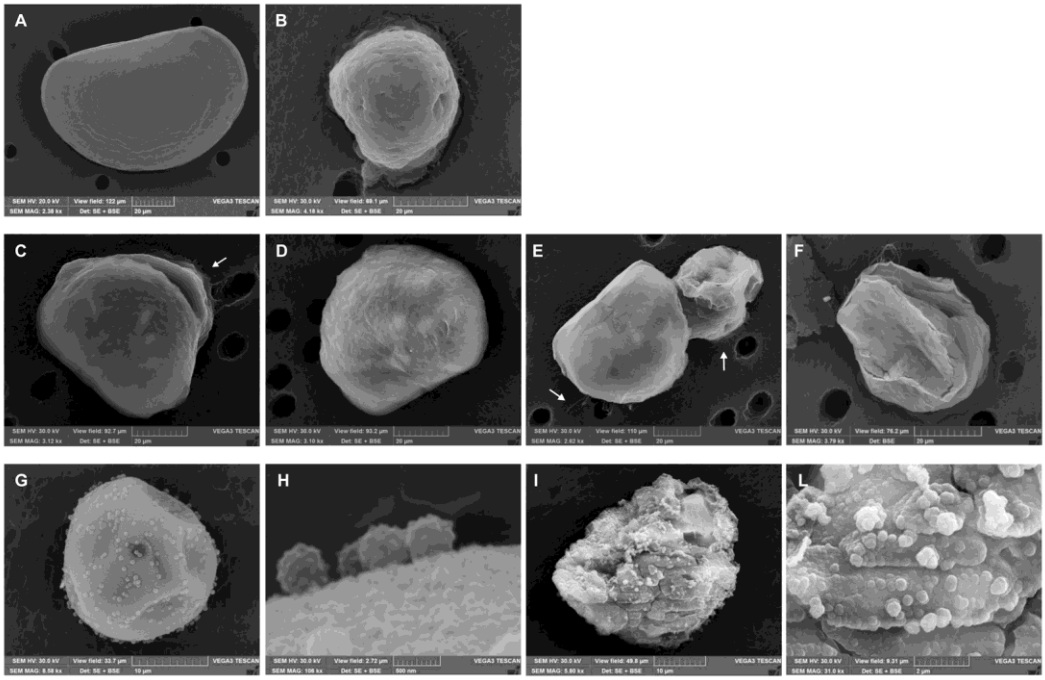

763 **Fig. S1**

Fig. S1

A) DLS analysis of PS-NH_2 suspensions (50 mg/L) in different media, showing Z-average (nm) and polydispersity index (PDI). Data are reported as mean ± SD. MQ: Milli-Q water; ASW: artificial sea water.

	Z-Average (nm)	PDI	ζ-potential (mV)
MQ	57	0.07	+42.8
ASW	200	0.30	+14.2

Representative images obtained by field emission scanning electron microscopy (FESEM) (B) and by TEM (C) on PS-NH_2 suspensions in ASW (20 mg/L).

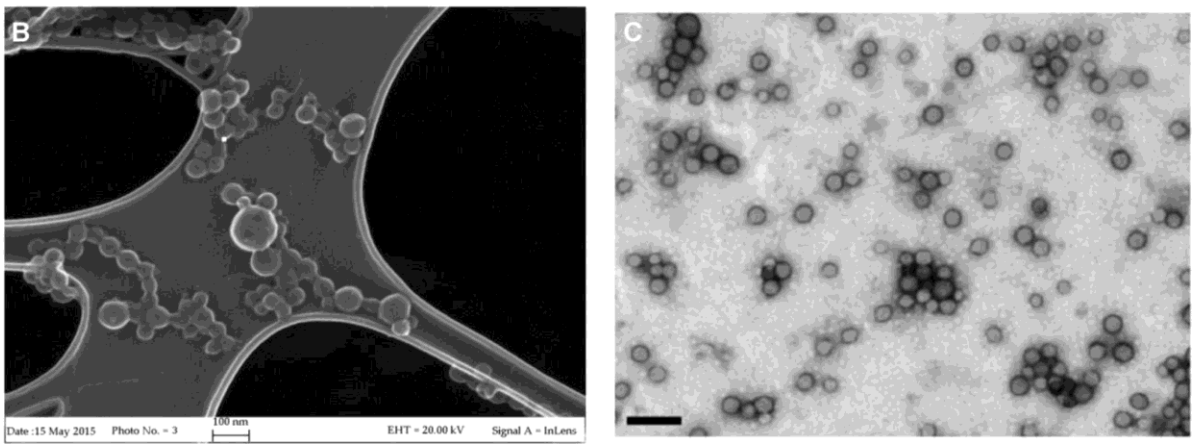

764

765

766

767

768

769

Fig. S2

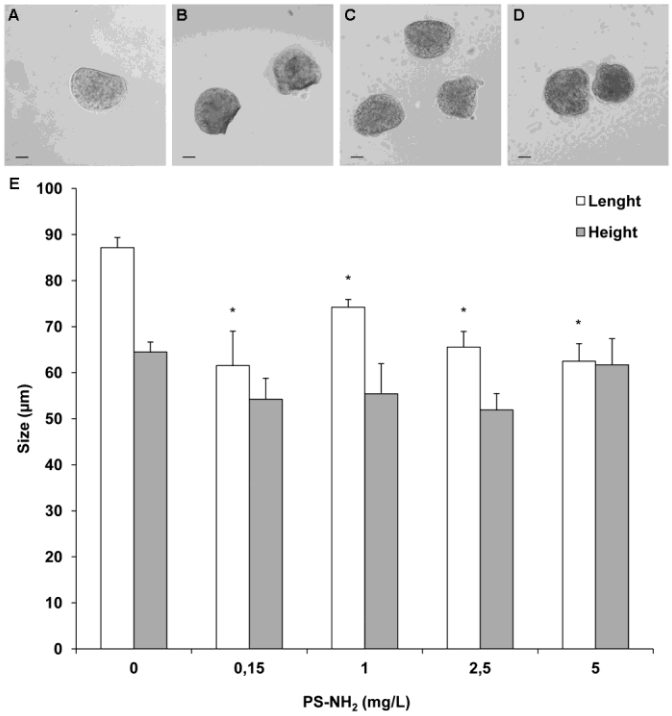

Fig. S3

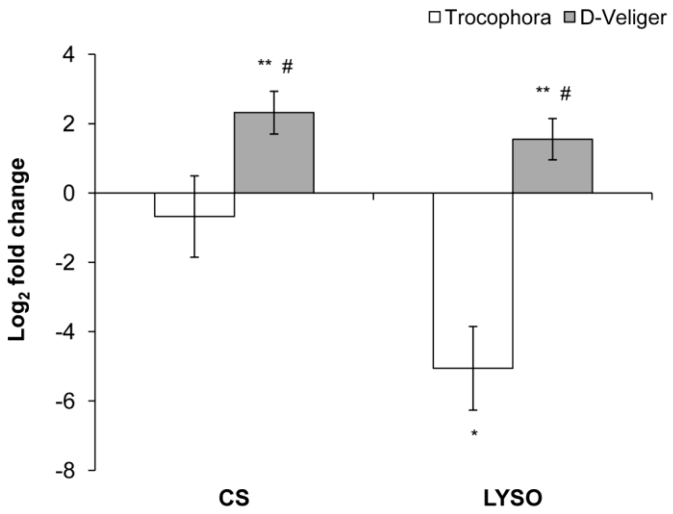

Fig. S4

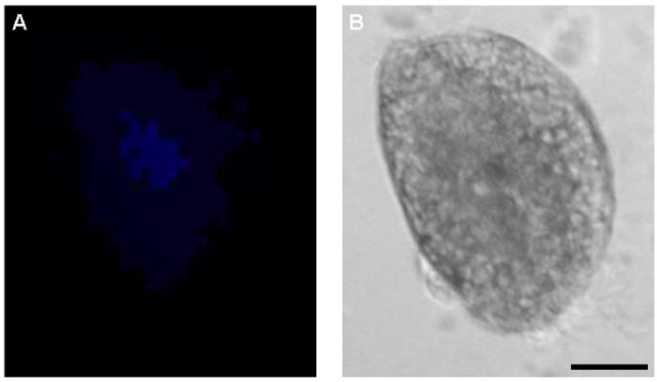

826 **Graphical abstract**

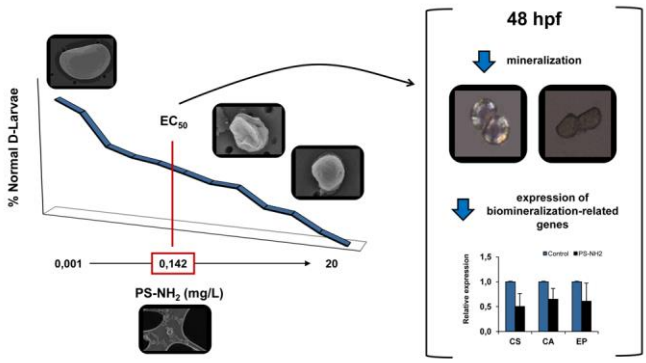

827